

Heat content of the Arabian Sea Mini Warm Pool is increasing

P. V. Nagamani,¹ M. M. Ali,^{1*} G. J. Goni,² T. V. S. Udaya Bhaskar,³ J. P. McCreary,⁴ R. A. Weller,⁵ M. Rajeevan,⁶ V. V. Gopala Krishna⁷ and J. C. Pezzullo⁸

¹National Remote Sensing Centre, ISRO, Hyderabad, India

²National Oceanic and Atmospheric Administration, AOML, Washington, DC, USA

³Indian National Center for Ocean Information Services, Hyderabad, India

⁴University of Hawaii, Honolulu, HI, USA

⁵Woods Hole Oceanographic Institution, Woods Hole, MA, USA

⁶Ministry of Earth Sciences, New Delhi, India

⁷National Institute of Oceanography, Goa, India

⁸Georgetown University, Washington, DC, USA

*Correspondence to:

M. M. Ali, Centre for
Ocean-Atmospheric Prediction
Studies, FSU, Tallahassee, FL,
USA

E-mail: mmali110@gmail.com

Abstract

Sea surface temperature in the Arabian Sea Mini Warm Pool has been suggested to be one of the factors that affects the Indian summer monsoon. In this paper, we analyze the annual ocean heat content (OHC) of this region during 1993–2010, using *in situ* data, satellite observations, and a model simulation. We find that OHC increases significantly in the region during this period relative to the north Indian Ocean, and propose that this increase could have caused the decrease in Indian Summer Monsoon Rainfall that occurred at the same time.

Keywords: tropical cyclone heat potential; Arabian Sea Mini Warm Pool; satellite altimetry; ocean heat content; all India monsoon rainfall

Received: 13 April 2013

Revised: 13 June 2015

Accepted: 4 July 2015

1. Introduction

The region in the southeastern Arabian Sea from 4°–14°N to 68°–78°E is referred to as the Arabian Sea Mini Warm Pool (ASMWP; Shenoi *et al.*, 1999). There, sea surface temperature (SST) exceeds 30 °C, 2–3 months before the onset of the Indian Summer Monsoon (Deepa *et al.*, 2007; Vinayachandran *et al.*, 2007; Vinayachandran and Kurian, 2008). A number of studies have explored the connection between the summer monsoon and ASMWP variables. For example, Joseph (1990), Rao and Sivakumar (1999), Deepa *et al.* (2007), Vinayachandran *et al.* (2007), and Sanil Kumar *et al.* (2004) investigated the impact of ASMWP SST on the summer-monsoon onset vortex. Rao and Sivakumar (1999) observed a direct correspondence between upper-ocean heat content (OHC) in the region from the ocean surface to the depth of the 28 °C isotherm during May–June and the genesis location of the onset vortex. Vinayachandran *et al.* (2007), however, concluded that, although the ASMWP impacts the onset vortex, it is not a sufficient condition for its formation. Rao *et al.* (2015) investigated the interannual variability of ASMWP variables in terms of their phase, amplitude, and spatial extent. Joseph (1990) suggested a need to study the ASMWP and its impact on the Indian Summer Monsoon Rainfall (ISMR).

In this study, we continue the effort to explore the relationship between the ASMWP and ISMR. Specifically, we show that ASMWP OHC has been increasing from 1993 to 2010, while ISMR has been decreasing at

the same time. This connection points toward a possible linkage between the two variables, with the increased OHC leading to a southward shift of atmospheric convection thereby weakening rainfall over India (see Section 4).

2. Data and methodology

As a measure of OHC, we use tropical cyclone heat potential (TCHP), which is similar to other OHC proxies except that it integrates temperature from the surface to the depth of the 26 °C isotherm instead of a fixed depth. We use three methods to calculate TCHP: a direct method using temperature profiles from *in situ* observations and model simulations through a numerical solution to version 3.1 of the Modular Ocean Model (MOM3.1), and an indirect one using satellite altimeter data.

In the first approach, we compute TCHP from the *in situ* and model profiles by,

$$\text{TCHP} = \rho C_p \int_0^{D_{26}} (T - 26) dz \quad (1)$$

where ρ is the sea water density, C_p is the specific heat capacity at constant pressure, $T(z)$ is ocean temperature (°C), and D_{26} is the depth of the 26 °C isotherm (Leipper and Volgenau, 1972). In this calculation, the product of ρC_p is taken as $4 \times 10^6 \text{ J K}^{-1} \text{ m}^{-3}$. Temperature profiles for Equation (1) are taken from observational data and MOM3.1 (courtesy: R. Sharma, 2013, pers. comm.).

The observed profiles are taken from all available temperature profiles during 1993–2010, namely, those collected during ship campaigns by conductivity temperature and depth (CTD) instruments, bathythermographs (BT), expendable BTs (XBT), and expendable CTDs (XCTD), as well as by Argo floats. All together 5761 *in situ* profiles (XBT – 2505, XCTD – 122, CTD – 356, Argo profiles – 2778) were considered during the study period. The model has been set up for the global domain (80°S–80°N) excluding polar regions, with a horizontal grid resolution varying from $0.58^\circ \times 0.58^\circ$ in the Indian Ocean to $2.8^\circ \times 2.8^\circ$ in the other oceans. There are 38 levels in the vertical, with 8 levels in the upper 40 m. The bottom topography is based on 1/12831/128 resolution data from the U.S. National Geophysical Data Center. Wind stress is computed from wind velocity using a wind-dependent, drag coefficient. Sharma *et al.* (2010) used this model to study the sea surface salinity variability. Temperature profiles from this model are used to compute TCHP as given in Equation (1).

If SST is less than 26°C, TCHP for the layer is assumed to be zero. If the temperature observation is not available at a depth of 26°C, D_{26} is determined by a linear interpolation. We retained only profiles with observations that begin at a depth of 5 m or less. As the Argo profiles do not have surface (0 m) observations, the shallowest observation (most profiles start from 4 m) is used for the surface value. We computed TCHP at all the locations within the region 4°–14°N and 68°–78°E, wherever *in situ* observations are available. The data used in plots are spatially and annually averaged TCHP values.

In the second approach, we use all the existing altimeter-derived, sea-surface-height anomaly (SSHA) data to determine TCHP (Goni *et al.*, 1996; Shay *et al.*, 2000). Accordingly, we assume, to first order, that the ocean can be approximated by a two-layer system with the upper-layer thickness (h_1) at latitude (x), longitude (y) and time (t). Then, provided that the mean upper-layer thickness (\bar{h}_1) and reduced gravity (g') fields are known from historical measurements, h_1 can be estimated from the altimeter-derived SSHA (η') field from

$$h_1(x, y, t) = \bar{h}_1(x, y) + \frac{g}{g'(x, y)} \eta'(x, y, t) \quad (2)$$

where $g' = \varepsilon g$, g is the acceleration of gravity and,

$$\varepsilon(x, y) = \frac{\rho_2(x, y) - \rho_1(x, y)}{\rho_2(x, y)} \quad (3)$$

where $\rho_1(x, y)$ and $\rho_2(x, y)$ represent upper- and lower-layer densities, respectively. Once the depth of the 26°C isotherm (h_1) is estimated, and SSHA is obtained from satellite observations, the TCHP is the excess heat contained above the 26°C isotherm. These TCHP values are obtained from Atlantic Oceanic and Meteorological Laboratory (AOML), National Oceanic and Atmospheric Administration (NOAA).

In addition, we analyzed SST trends from Tropical Rainfall Measuring Mission Microwave Imager

during 1997–2010 and net heat flux from OAFflux (Yu *et al.*, 2007) during 1993–2009. All these observations are annually averaged. We also examined ISMR data from 1993 to 2010 obtained from India Meteorological Department (IMD). Total all India rainfall during the monsoon period, June–September, is used in this study.

3. Results

The comparison between *in situ* and satellite-derived TCHP shows a bias (*in situ* values being on the higher side) of 8.9 kJ cm^{-2} with a coefficient of determination, R^2 , of 0.82 and root mean square error (RMSE) of 9.4 kJ cm^{-2} (Figure 1). Nagamani *et al.* (2012) compared the two estimations over the entire north Indian Ocean (NIO) and found an RMSE of 20.95 kJ cm^{-2} with an R^2 of 0.65 and bias of 11.27 kJ cm^{-2} .

During 1993–2010, the OHC of the region increased from 70.5 kJ cm^{-2} (61 kJ cm^{-2}) to 85 kJ cm^{-2} (78 kJ cm^{-2}), with an overall warming of 14.5 kJ cm^{-2} (17 kJ cm^{-2}) in the *in situ* (satellite) observations (Figure 2). These increasing OHC trends are statistically significant, with a p value of 0.002 (i.e., the probability p that there is no trend is less than 0.2%). Using the temperature profiles from MOM3.1, there is an overall increase of 20.5 kJ cm^{-2} during this period (from 42.5 kJ cm^{-2} in 1993 to 63 kJ cm^{-2} in 2010). Though the model results show higher warming compared to satellite and *in situ* observations, the slope is highly significant ($p < 0.001$) with R^2 of 0.565 between the year and OHC. Although the *in situ*, model and satellite observations have biases, all the three observations show an increasing trend. It is noteworthy that such large increasing trends are not observed in other parts of the NIO, although Roxy *et al.* (2014) observed an overall warming trend in the entire NIO. For example, satellite-derived OHC increased by only 3.5 kJ cm^{-2} in the Bay of Bengal and decreased by about 1 kJ cm^{-2} in the rest of the Arabian Sea (i.e. outside the ASMWP).

The increasing trend in ASMWP heat content is consistent with SST changes in the region. On the average, SST increased from 28.4 to 28.9°C during 1993–2010. If the average temperature of this column were equal to SST, OHC of the column would increase by 22.4 kJ cm^{-2} over an 80-m thick upper layer (the average depth of the 26°C isotherm). As the average temperature this column is generally less than SST owing to mixing processes, the estimated increase in OHC could be slightly less as well. At the same time, the net surface heat flux (NHf) in the ASMWP decreased by 24 W m^{-2} (Figure 3), a reduction that reduces the OHC of an 80-m water column by 34 kJ cm^{-2} . Thus, the net increase in OHC due to the changes in both SST and NHf is slightly less than 19.44 kJ cm^{-2} , which is closer to 17 kJ cm^{-2} of the estimation from satellite observation, if the ocean mean temperature is considered to be less than SST. Even these calculations suggest the

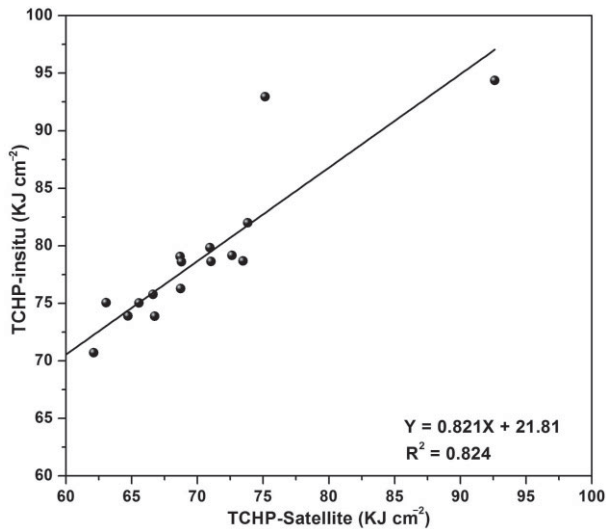


Figure 1. Comparison of *in situ* and satellite-derived OHC over the Arabian Sea Mini Warm Pool region during 1993–2010. The slope of the regression line is found to be significantly non-zero at the 95% level ($p < 0.001$).

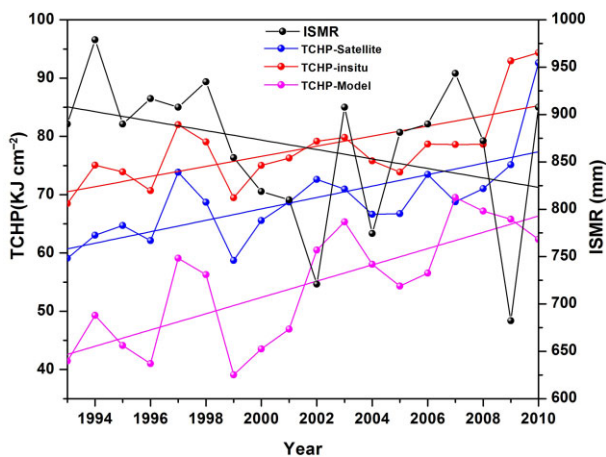


Figure 2. Comparison of Indian Summer Monsoon Rainfall (green dots and line) with tropical cyclone heat potential over the Arabian Sea Mini Warm Pool region from (a) *in situ* (red dots and line), (b) satellite (blue dots and line) and (c) model (pink dots and line) observations during 1993–2010.

increase in OHC of the region. However, the changes in OHC are due to a combination of surface fluxes and internal heat changes due to advection.

It is noteworthy that ISMR dropped from 910 to 820 mm during 1993–2010 (Figure 2), although the trend is not statistically significant ($p = 0.230$), suggesting that there is an inverse relationship between ISMR and ASMWP OHC. Such a linkage is possible as follows: Increased OHC and SST in the ASMWP lead to enhanced convection there, thereby shifting convection southward that would normally occur farther north and, hence, weakening the tropical easterly jet stream (Abish *et al.*, 2013) and ISMR. Earlier, Chung and Ramanathan (2006), using version 3 of the Community Climate Model, attributed a reduction in monsoon rainfall in their solution to an increase of equatorial SST; specifically, they report that the reduction in

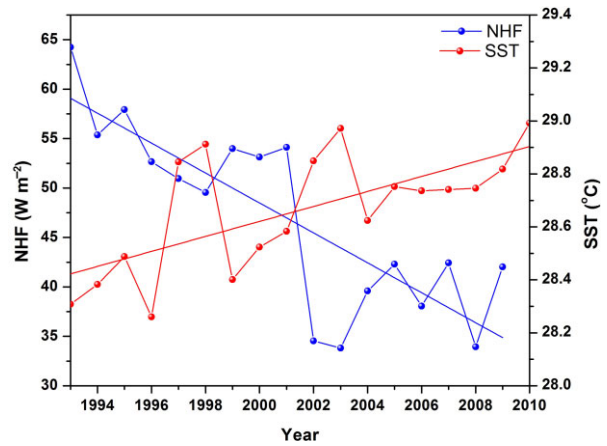


Figure 3. Trends in net heat flux (NHF, in blue) and sea surface temperature (SST, in red) during 1993–2009 for NHF (we did not have access beyond 2009) and 1993–2010 for SST.

the temperature difference averaged from 60°–100°E between the equator and the 25°N reduces monsoon rainfall. We suggest that the increase in OHC of the study region covering 4°–14°N and 68°–78°E was a significant factor in reducing the northward SST gradient. However, until a detailed modeling study, is carried out to confirm this idea, this relation is speculative.

4. Summary and discussion

The major emphasis of this paper is to show that the annual average TCHP of the study region is increasing. The ASMWP is known to impact the summer monsoon through its influence on the location of the monsoon onset vortex. Using *in situ* observations, satellite estimations, and model simulations, we show that OHC (and SST) in the ASMWP increased during 1993–2010 while ISMR decreased. Further, we suggest that the former leads to the latter by weakening the northward temperature gradient and, hence, allowing shifting convection southward. Here, we propose a possible linkage. More detailed modeling affords are required to prove this, which is beyond the scope of this study.

We recognize that other factors also affect ISMR, and therefore blur (and possibly overwhelm) any connection to ASMWP OHC. These factors include: increased aerosols, regional SST and OHC changes elsewhere in the Indian Ocean, and ‘noise’ due to climate variability such as El Nino Southern Oscillations (ENSO) and the Indian Ocean Dipole (IOD). Regarding the impact of aerosols, some studies suggest black carbon (Ramanathan *et al.*, 2005) or sulfate (Bollasina *et al.*, 2011) aerosols mask surface warming and the resulting cooler SST decreases monsoon rainfall, whereas, Wang (2004) draws the opposite conclusion. Regarding the impact of other regions of SST and OHC anomalies, Annamalai *et al.* (2013) noted the importance of regional heat sources over the Asian monsoon region, concluding that dynamical feedbacks among

them complicate the hypothesis that increased ocean temperatures increase tropospheric moisture and hence rainfall. Further, Swapna *et al.* (2013) noted the importance of warming in the equatorial IO, concluding that the weakening of the summer monsoon circulation accelerated the warming of the equatorial IO, and that this warming in turn contributed to a further weakening of the monsoon with more monsoon breaks. When this small region can have a relation with the onset of the Southwest monsoon (which is proved through several publications), we suggest that OHC of the ASMWP could also be one of the factors that impact ISMR. Since we studied the overall annual trend in TCHP, we have not isolated the seasonal changes. This increase, as a part of the climatic trend, is possibly reducing the summer monsoon rainfall because the TCHP affects the atmosphere only at the time of the year when convection is possible at all, that is during the summer. In addition, the summer-averaged TCHP signal compares well with the annually averaged one. To confirm this property, we compared the satellite-derived TCHP during June to September with its 12-month average value. The comparison has a bias of 20 kJ cm^{-2} (June–September OHC being less than annual value) with a Pearson's correlation coefficient of 0.8, indicating that even the June-to-September TCHP is also increasing similar to the annual value, over the study period. (We are aware that TCHP during this season alone need not influence the Indian summer monsoon.)

In conclusion, our study suggests the importance of further investigation in to the influence of the ASMWP heat content on monsoon dynamics. It points toward the need for a sustained observational effort that allows the statistical relationship between OHC and Indian rainfall to be accurately determined. Further, it suggests the need for comprehensive modeling studies to demonstrate the dynamical processes involved in this linkage.

Acknowledgements

The authors acknowledge the TCHP data from AOML, NOAA, *in situ* temperature profiles from Indian National Centre for Ocean Information Services, rainfall data from India Meteorological Department, SST from remote sensing systems, and flux observations from Woods Hole Oceanographic Institution. The authors thank Dr Rashmi Sharma, Space Applications Centre for providing the TCHP values from the MOM-3.1 model. The support and encouragement provided at the respective organizations are gratefully acknowledged. The authors have no conflict of interest.

References

Abish B, Joseph PV, Johannessen OM. 2013. Weakening trend of the tropical easterly jet stream of the boreal summer monsoon season 1950–2009. *Journal of Climate* **26**: 9408–9414.

- Annamalai H, Hfner J, Sooraj KP, Pillai P. 2013. Global warming shifts the monsoon circulation drying south Asia. *Journal of Climate* **26**: 2701–2718.
- Bollasina MA, Yi M, Ramaswamy V. 2011. Anthropogenic aerosols and the weakening of the south Asian summer monsoon. *Science* **334**: 502–504.
- Chung CE, Ramanathan V. 2006. Weakening of North Indian SST gradients and the monsoon rainfall in India and the Sahel. *Journal of Climate* **13**: 2036–2045.
- Deepa R, Seetaramayya P, Nagar SG, Gnanaseelan C. 2007. On the plausible reasons for the formation of onset vortex in the presence of the Arabian Sea mini warm pool. *Current Science* **92**: 794–800.
- Goni G, Kamholz S, Garzoli S, Olson D. 1996. Dynamics of the Brazil-Malvinas confluence based on inverted echo sounders and altimetry. *Journal of Geophysical Research* **101**(C7): 16273–16289.
- Joseph PV. 1990. Warm pool over the Indian Ocean and monsoon onset. *Tropical Ocean Global Atmosphere Newsletters* **53**: 1–5.
- Leipper D, Volgenau D. 1972. Hurricane heat potential of the Gulf of Mexico. *Journal of Physical Oceanography* **2**: 218–224.
- Nagamani PV, Ali MM, Goni GJ, Dinezio PN, Pezzullo JC, Udaya Bhaskar TVS, Gopalakrishna VV, Kurian N. 2012. Validation of satellite-derived tropical cyclone heat potential with *in situ* observations in the north Indian Ocean. *Remote Sensing Letters* **3**(7): 615–620.
- Ramanathan V, Chung C, Kim D, Bettge T, Buja L, Kiehl JT, Washington WM, Fu Q, Sikka DR, Wild M. 2005. Atmospheric brown clouds: impacts on South Asian climate and hydrological cycle. *Proceedings of the National Academy of Sciences of the United States of America* **102**: 5326–5333.
- Rao RR, Sivakumar R. 1999. On the possible mechanisms of the evolution of a mini-warm pool during the pre-summer monsoon season and the onset vortex in the southeastern Arabian Sea. *Quarterly Journal of the Royal Meteorological Society* **125**: 787–809.
- Rao RR, Jitendra V, GirishKumar MS, Ravichandran M, Ramakrishna SSVS. 2015. Interannual variability of the Arabian Sea Warm Pool: observations and governing mechanisms. *Climate Dynamics* **44**(7–8): 2119–2136.
- Roxy M, Kapoor R, Terray P, Masson S. 2014. Curious case of Indian Ocean warming. *Journal of Climate* **27**: 8501–8509, doi: 10.1175/JCLI-D-14-00471.1.
- Sanil Kumar KV, Hareesh Kumar PV, Joseph J, Panigrahi JK. 2004. Arabian Sea mini warm pool during May 2000. *Current Science* **86**: 180–184.
- Sharma R, Agarwal N, Momin IM, Basu S, Agarwal VK. 2010. Simulated sea surface salinity variability in the tropical Indian Ocean. *Journal of Climate* **23**: 6542–6554.
- Shay LK, Goni GJ, Black PG. 2000. Effect of a warm ocean ring on hurricane Opal. *Monthly Weather Review* **128**: 1366–1383.
- Shenoi SSC, Shankar D, Shetye SR. 1999. On the sea surface temperature high in the Lakshadweep Sea before the onset of the southwest monsoon. *Journal of Geophysical Research* **104**: 15703–15712.
- Swapna P, Krishnan R, Wallace JM. 2013. Indian Ocean and monsoon coupled interactions in a warming environment. *Climate Dynamics* **42**(9–10): 2439–2454, doi: 10.1007/s00382-013-1787-8.
- Vinaychandran PN, Kurian J. 2008. Modeling Indian Ocean circulation: Bay of Bengal fresh plume and Arabian Sea min warm pool. In *Proceedings of the 12th Asian Congress of Fluid Mechanics*, Daejeon, Korea, 18–21 August 2008.
- Vinaychandran PN, Shankar D, Kurian J, Durand F, Shenoi SSC. 2007. Arabian Sea mini warm pool and the monsoon onset vortex. *Current Science* **93**(2): 203–214.
- Wang CA. 2004. A modeling study on the climate impacts of black carbon aerosols. *Journal of Geophysical Research* **109**: D03106, doi: 10.1029/2003jd004084.
- Yu L, Jin X, Weller RA. 2007. Annual, seasonal, and inter annual variability of air–sea heat fluxes in the Indian Ocean. *Journal of Climate* **20**: 3190–3209.